NANO LETTERS

Letter

pubs.acs.org/NanoLett

Atomically Wired Molecular Junctions: Connecting a Single Organic Molecule by Chains of Metal Atoms

Tamar Yelin,[†,#] Ran Vardimon,[†,#] Natalia Kuritz,[†,‡] Richard Korytár,[§] Alexei Bagrets,[§,∥] Ferdinand Evers,[§,⊥] Leeor Kronik,[‡] and Oren Tal*[,†]

[†]Department of Chemical Physics and [‡]Department of Materials and Interfaces, Weizmann Institute of Science, Rehovot, 76100 Israel
[§]Institute of Nanotechnology, [∥]Steinbuch Centre for Computing, and [⊥]Institut Für Theorie der Kondensierten Materie, Karlsruhe Institute of Technology (KIT), 76128 Karlsruhe, Germany

Supporting Information

ABSTRACT: Using a break junction technique, we find a clear signature for the formation of conducting hybrid junctions composed of a single organic molecule (benzene, naphthalene, or anthracene) connected to chains of platinum atoms. The hybrid junctions exhibit metallic-like conductance ($\sim 0.1-1 G_0$), which is rather insensitive to further elongation by additional atoms. At low bias voltage the hybrid junctions can be elongated significantly beyond the length of the bare atomic chains. Ab initio calculations reveal that benzene based hybrid junctions have a significant binding energy and high structural flexibility that may contribute to the survival of the hybrid junction during the elongation process. The fabrication of hybrid junctions opens the way for combining the different properties of atomic chains and organic molecules to realize a new class of atomic scale interfaces.

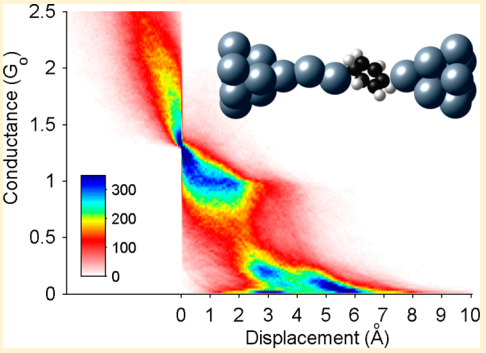

KEYWORDS: *Single molecule, molecular junction, break junction, atomic chain, oligoacene, electron transport*

Acquiring control over electronic transport at the atomic scale requires the ability to fabricate electronic devices in atomic resolution. The high level of control over the atomic structure of organic molecules promoted the use of molecular junctions as a test bed for electronic transport at the atomic scale.[1−6] However, the structure of these junctions is limited to a molecule sandwiched between macro-scale electrodes with typical conductance restricted to off-resonance tunneling (several orders of magnitude lower than G_0). Ideally, one would like to have the freedom to wire individual organic molecules to other atomic-scale conductors[7−9] with minimal conductance attenuation in order to form efficient molecular junctions based on more than a single atomic-scale component. Here we show that benzene and larger organic molecules can be electrically connected by the smallest possible conducting wire: a chain of atoms. The wiring process is done in a mechanically controllable break junction setup by pulling atom after atom from platinum (Pt) electrodes into a molecular junction.

When atomic chains are pulled between metallic electrodes in the presence of diatomic molecules, the chains can be decorated by the small molecules or their decomposed atoms.[10−15] In the case of organic molecules connected by thiol groups between two gold electrodes, stretching the junction can lead to its elongation.[16−19] A direct binding of alkanes to gold electrodes showed similar behavior.[20] In these cases, however, it is not trivial to determine whether the observed elongation is a consequence of atomic chains being pulled from the electrodes or simply a collective deformation of the electrode apexes.[16,21] These junctions are typically characterized by low conductance due to the linking groups at the molecule−electrode interfaces[16−19,22] or the susceptibility of the conductance to molecular length.[20] We show that binding organic molecules such as benzene, naphthalene, or anthracene directly to Pt electrodes, can form highly conductive hybrid junctions (HJs) with atomic chains bridging the organic molecule and the electrodes. All three HJs have a comparable conductance which is weakly dependent on the chain length. The conditions for the formation of HJs can be optimized to have longer chains than obtained by stretching bare atomic Pt junctions. Ab initio calculations show that wiring benzene with Pt atomic chains leads to a stable molecular junction with significant structural flexibility. Further analysis indicates that the Pt-benzene bond is formed by hybridization between the benzene π-orbitals and the Pt d-orbitals.

The HJs were constructed using a mechanically controllable break junction[23] (Figure 1b, inset) operated at 4.2K. After breaking a Pt wire in cryogenic vacuum to form two ultraclean electrode tips, the target molecules were introduced via a heated capillary[24] that forms a passage between a molecular source at room temperature and the cold Pt junction. Conductance (I/V) was measured as a function of relative electrode displacement as the junction was broken and

Received: December 20, 2012
Revised: March 4, 2013

   dx.doi.org/10.1021/nl304702z | *Nano Lett.* XXXX, XXX, XXX−XXX

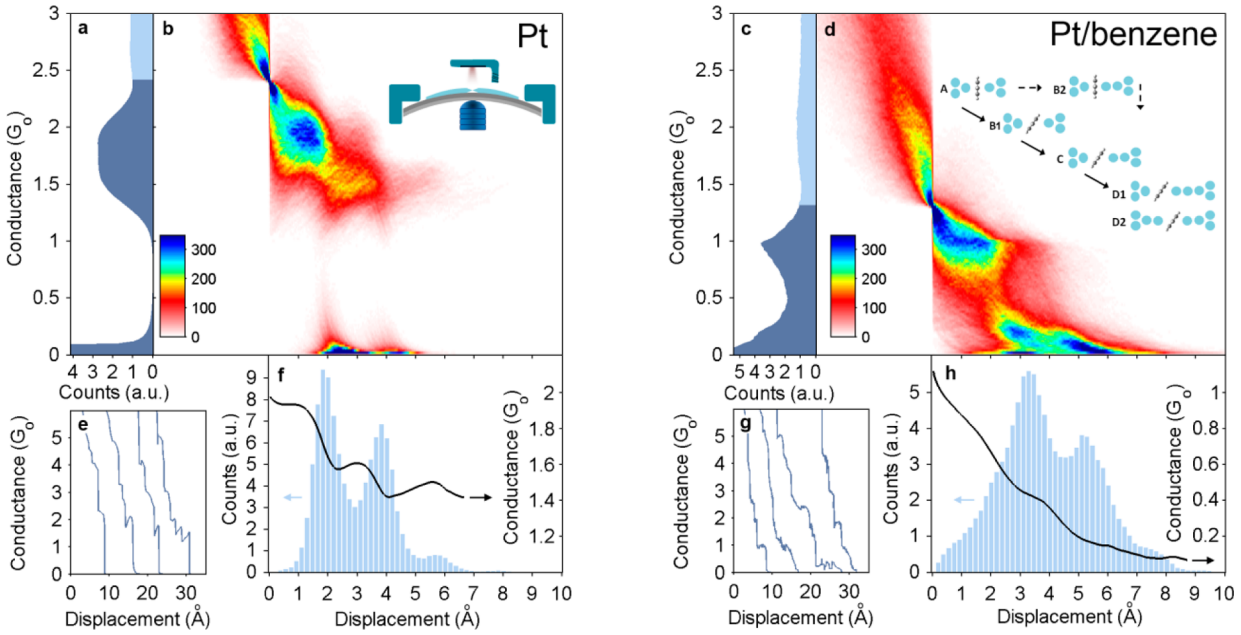

Figure 1. Statistical analysis of 10 000 conductance traces measured before and after the introduction of benzene to Pt junctions (left and right panel, respectively). (a, c) Conductance histograms. The peaks represent the most probable conductance of atomic and single molecule junctions, respectively. (b, d) 2D histograms of the number of counts at each conductance−displacement combination. Zero displacement is set to a fixed conductance value ($2.4G_0$ for Pt, $1.3G_0$ for Pt/benzene) chosen at the top edge of the peak in the conductance histogram. Insets: mechanically controllable break junction apparatus (b) and artist's impression of the evolution of Pt/benzene HJ during stretching (d). (e, g) Examples for conductance traces, shifted for clarity. (f, h) Length histograms (light blue) showing the distribution of junction lengths from zero displacement until rupture (see Supplementary Sections 2,3) and average conductance traces (black curves) showing the evolution of the conductance during stretching. All of the measurements presented in this figure were taken at a bias voltage of 100 mV.

reformed repeatedly in order to collect statistical data. Additional experimental details are discussed in the Supporting Information.

As a first step, benzene was introduced to a bare Pt junction.[24] As a result, a clear change in the junction conductance was observed, indicating the formation of a Pt/benzene junction. Figure 1e shows several conductance traces measured during breaking of a Pt wire prior to benzene introduction. The last conductance plateau before rupture is attributed to conductance through a cross section of a single atom.[25] The conductance histogram in Figure 1a was constructed from a set of 10 000 conductance traces. The broad peak at $\sim 1.7G_0$, where $G_0 = 2e^2/h$ is the conductance quantum, indicates the most probable conductance of a single atom constriction, and the tail-shaped distribution at low conductance is the signature of tunneling transport that follows the rupture of atomic contacts.[9,26,27] When benzene is introduced the conductance histogram changes considerably[28,24] (Figure 1c). The peak at $\sim 1.7G_0$ vanishes, and a new conductance peak appears at $\sim 1.0G_0$, accompanied by a pronounced tail at lower conductance. This somewhat lower conductance of the molecular junctions is also apparent when comparing individual traces (Figure 1e,g). Using inelastic electron spectroscopy, the formation of molecular junctions is verified independently, as seen in Supplementary Section 4.

To learn about the structure of the Pt/benzene junctions when the electrode separation is increased, the same set of traces was used to construct a 2D histogram (Figure 1d). Here the color code represents the number of times that a certain combination of conductance and relative electrode displacement was detected. The observed decrease in conductance from $\sim 1G_0$ to $0.2G_0$ as the junction is elongated by ~ 3 Å is in good agreement with previous findings by Kiguchi et al.[28] that attributed this conductance reduction to a transition from a perpendicular orientation to a tilted orientation of the benzene molecule in the junction (Figure 1d, A and B1, respectively).

Surprisingly, the Pt/benzene junction is elongated significantly beyond the typical length of an extended Pt−benzene−Pt junction (~ 3 Å elongation in Figure 1d).[28] To better understand this observation, we studied the distribution of lengths that the junctions can be elongated to. We constructed a length histogram (Figure 1h) from 10 000 independent molecular junctions (see Supplementary Sections 2,3). The sequence of peaks shows that the junction can have several typical length values, indicating that the junction is elongated each time by a similar repeated unit with a length equal to the distance between the peaks.[9] The average peak separation is 2.0 ± 0.3 Å. Interestingly, the peak separation is similar to the typical repeated unit found for Pt atomic chains.[9,26] Smit et al.[9] showed that atomic chains can be formed when Pt atomic junctions are elongated. When the distance between the electrodes increases, the junction can either break (revealed as a series of conductance drops in Figure 1b) or be elongated by pulling an atom from the electrodes. The process can repeat itself to form a chain of several atoms. Figure 1f shows a length histogram constructed from conductance traces that were measured for a bare Pt junction right before the introduction of benzene. The sequence of peaks presented here is the signature of Pt atomic chain formation,[9] and the average peak separation is 2.0 ± 0.2 Å, similar to the value found for the elongated Pt/benzene junction. This indicates that the Pt/benzene junction is most likely elongated by sequential addition of Pt atoms to the molecular junction.

dx.doi.org/10.1021/nl304702z | Nano Lett. XXXX, XXX, XXX−XXX

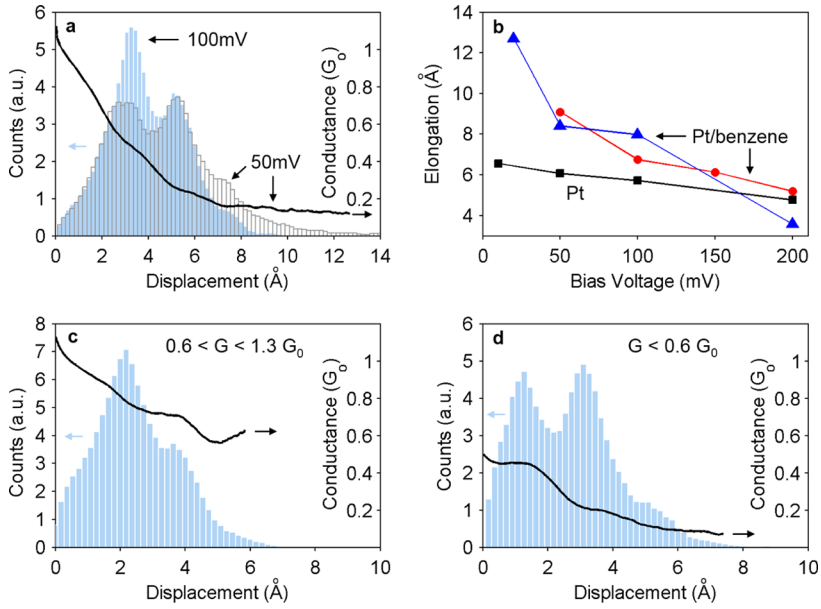

Figure 2. (a) Length histograms for Pt/benzene junctions constructed from 10 000 traces each, measured in two sequential measurements at 50 mV (dark gray) and 100 mV bias voltage (light blue). The length histogram is extended to higher displacement values for the lower bias voltage. The average conductance trace (black curve) is based on measurements at 50 mV bias. (b) Length dependence on bias voltage of Pt (squares) and Pt/benzene (circles and triangles) junctions. Each point represents the average length of the longest 10% atomic or molecular junctions and the lines connect sequential points. For Pt/benzene two sequences of measurements are presented. (c, d) Length histograms and average conductance traces measured at 100 mV, constructed from the part of each trace inside a conductance window of $1.3-0.6G_0$ (c) and lower than $0.6G_0$ (d).

To verify that the repeated unit is indeed a Pt atom, we looked for an additional fingerprint of Pt atomic chains. We compared the average conductance as a function of electrode displacement for sets of traces measured before and after the introduction of benzene (black curves in Figure 1f,h, respectively). The average conductance trace of Pt junctions reveals oscillations with the same periodicity of the peaks in the length histogram.[29] These oscillations were attributed to repeated transitions between a zigzag to a more linear configuration as the chain is elongated.[30] The chain straightening leads to a better orbital overlap which allows for higher conductance. Further stretching eventually reduces the conductance due to substantial interatomic separation before another atom is pulled in or due to chain rupture. The average trace of Pt/benzene junctions (Figure 1h) reveals clear conductance oscillations on top of the overall reduction in conductance. The periodicity of the oscillations is remarkably similar for Pt and Pt/benzene junctions. This additional indication for the presence of Pt atomic chains provides further verification for the formation of hybrids based on molecules and atomic chains. We do not find indications for adsorption of additional molecules on the HJ, such as larger peak separation in the length histogram when molecules are introduced, as previously found for Pt chains exposed to hydrogen.[11] In the latter case, the larger peak separation was ascribed to larger Pt–Pt atomic distance due to chain decoration by hydrogen. Our observation is insensitive to the molecule dosage.

The elongation of benzene HJs can be improved significantly by the right choice of applied voltage across the junction. Figure 2a shows length histograms of benzene HJs, measured at bias voltage of 50 mV and 100 mV. The length histogram taken at 50 mV reflects a higher probability for the formation of longer HJs while the location of the peaks remains roughly the same. The effect of the applied voltage on the chain length is a general trend as seen in Figure 2b. Here, the average length of the longest 10% of the traces is presented as a function of applied voltage. The maximal elongation of bare Pt junctions is only moderately affected by the applied voltage in the presented range. On the other hand, the longest Pt/benzene traces become substantially longer at lower voltage. The different dependence can be understood as a consequence of different sensitivity to heating effects such as Joule heating and voltage excitation of vibrations in the junction,[31−35] as well as current-induced forces.[36,37] The onset of vibration activation of Pt/benzene junctions takes place between 20 and 50 mV.[24] Interestingly, this is the range of voltages in Figure 2b which exhibits the largest difference in the behavior of the Pt and Pt/benzene junctions. Therefore, the higher sensitivity of Pt/benzene junctions to the applied voltage can be attributed to the activation of molecular junction vibrations. In addition to the stronger length-voltage dependence, at low bias voltage the length of benzene HJs is remarkably higher than the length of bare Pt chains. This exceptional stability of the HJs is not fully understood. However, the richness of possible configurations of HJs compared to the homogeneous Pt chains may play an important role in their remarkable survival under elongation.

We now examine the evolution of conductance with junction elongation. As mentioned above, when the junction is stretched the conductance decreases from $1G_0$ to $0.2G_0$. This behavior was previously ascribed to molecule tilting.[28] However, in Figure 1d we can recognize a plateau at $\sim 1G_0$ which coexists with the general trend of conductance decrease. Constructing a length histogram and an average trace (Figure 2c) for the high conductance region ($1.3-0.6G_0$) reveals peaks in the length histogram separated by 1.7 ± 0.3 Å and oscillations in the average conductance. These observations indicate that HJs can be formed in a secondary scenario (relevant for ~20% of the traces) with no significant conductance reduction and probably with no substantial molecule tilting (illustrated in Figure 1d,

dx.doi.org/10.1021/nl304702z | Nano Lett. XXXX, XXX, XXX−XXX

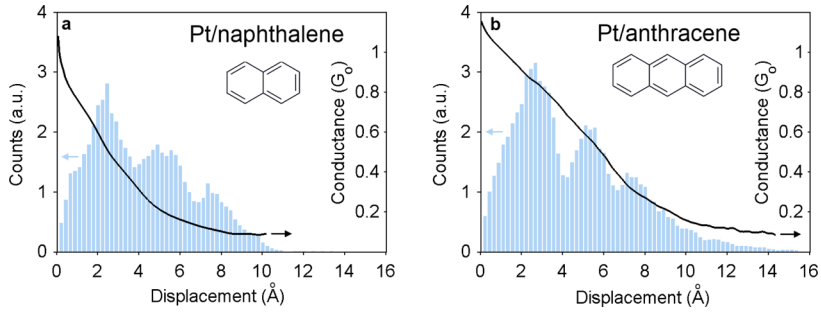

Figure 3. (a) Length histograms (light blue) and average conductance traces (black curves) of Pt/naphthalene (a) and Pt/anthracene (b) junctions, both measured at 200 mV bias voltage and constructed from more than 5000 traces.

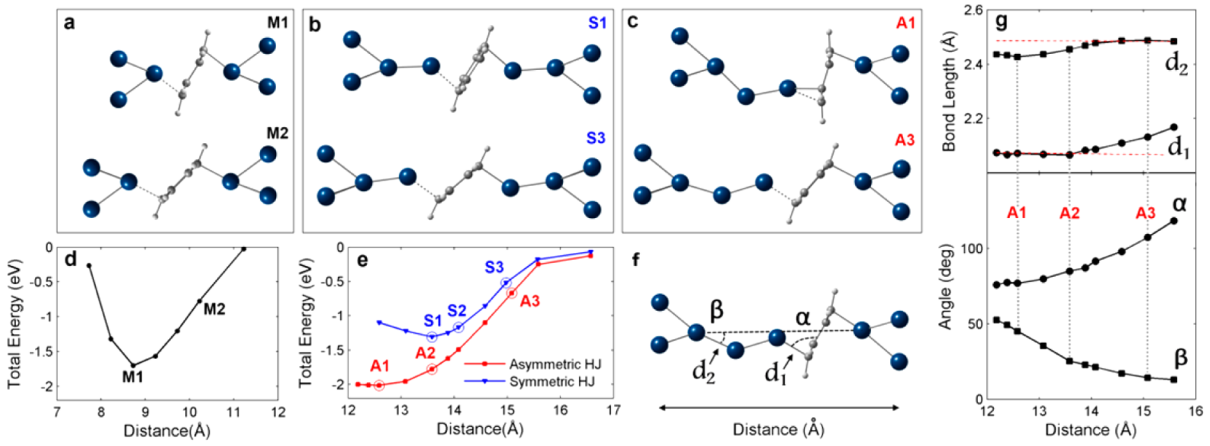

Figure 4. (a, b, c) Optimized geometries of Pt/benzene junctions calculated for different electrode distances to illustrate possible snapshots during junction stretching. Three possible cases are treated: molecular junction with no additional atoms (a), symmetric HJ with one additional atom at each side (b), and asymmetric HJ with two additional atoms at one side (c). For each case, the most stable and a stretched configuration are shown (top and bottom, respectively). The structures were obtained by fixing the distance between the electrodes while optimizing the positions of the molecule, the additional atoms, and the atom at the apex of each electrode. (d, e) Total energy plots showing the calculated total energy for the relaxed structures at each interelectrode distance for the molecular junction (d) and the symmetric and asymmetric HJs (e). The total energies are presented relative to the corresponding ruptured junction, obtained by splitting the junctions at the bond prone to rupture (according to force analysis), marked in a, b, and c by dashed lines. (f) Definitions of relevant bond lengths and angles of the asymmetric HJ (shown in c). (g) Evolution of the defined bond lengths and angles of the asymmetric HJ as a function of interelectrode distance.

B2). Eventually, all traces drop to the low conductance region, below $0.6G_0$, where they can be further elongated (Figure 2d).

Focusing on the average conductance at high displacement (beyond 5 Å in Figure 2d), a very moderate conductance dependence on elongation is observed. This tendency is better seen for measurements taken at 50 mV bias (Figure 2a, black curve) because the junction elongation is enhanced. Here, beyond the initial conductance reduction, an insignificant conductance dependence on length is clearly observed, indicating a remarkable insensitivity of the average conductance to the introduction of additional Pt atoms.

To test whether other organic molecules can form HJs by binding to Pt electrodes, we performed similar experiments with naphthalene and anthracene. Figure 3 presents length histograms and average traces for Pt/naphthalene and Pt/anthracene molecular junctions. In both cases the junctions are elongated significantly beyond the molecule length (which is roughly 5 Å and 7 Å, respectively[38]). The series of peaks in the length histograms indicates a repeated unit that adds up as the junction is elongated. In comparison to Pt/benzene HJs, the length histograms of naphthalene and anthracene junctions have a higher number of peaks, which indicates that HJs based on these molecules can form hybrids with longer atomic chains. The larger average peak separation found for these junctions (2.4 ± 0.3 and 2.2 ± 0.3 Å, respectively) can result from more effective rearrangement (e.g., tilting or sliding) of the longer molecules that permits an extended elongation before rupture or insertion of an additional atom. Conductance oscillations can be seen in both cases, although they are more pronounced for Pt/naphthalene. These findings clearly indicate that the formation of stable HJs is possible for different organic molecules and should be further tested as a more general method for wiring organic molecules with atomic chains.

To better understand the structure and stability of benzene-based HJs, we performed DFT calculations using the Quantum Espresso[39] package (see Supplementary Section 6). We note that our calculations are at equilibrium and therefore do not address the effect of bias. Figure 4a shows two optimized configurations of a benzene junction with no chain atoms. The benzene tilt is seen when comparing the most stable configuration (M1) and a stretched configuration before rupture (M2). Figure 4d shows the total energy change as the electrodes are pulled apart. The binding energy of the junction, determined by the difference between the total energy of the most stable configuration and of the ruptured junction, is 1.7 ± 0.1 eV. This value indicates significantly stronger binding than a typical physical adsorption, in agreement with previous findings.[28] Note that the calculated Pt−C bond length is about

dx.doi.org/10.1021/nl304702z | Nano Lett. XXXX, XXX, XXX−XXX

2.1 Å, typical to chemical binding. In Figure 4e the total energy for symmetric and asymmetric HJs with two chain atoms is plotted versus electrode displacement (sample configurations shown in Figure 4b,c). For the asymmetric HJ the energy does not increase substantially beyond the most stable configuration due to a low barrier transition to a more compact configuration. The better energetic stability of the asymmetric junction with respect to the symmetric one is manifested in the binding energies: 2.0 ± 0.1 eV and 1.3 eV ± 0.1 eV, respectively. Interestingly, inelastic electron spectroscopy (see Supplementary Section 4) is consistent with asymmetric coupling to the electrodes.

The stability of benzene HJs during stretching is facilitated by the additional degrees of freedom in which the HJ can be modified to survive elongation. This is illustrated in Figure 4f,g for the asymmetric structure. The length of the bond prone to rupture between the molecule and the chain (d_1), as well as the angle between this bond and the molecule (α) are only moderately increased for a substantial stretching distance (up to point A2) while the chain becomes more linear and the angle between the chain and the electrode axis (β) is considerably modified. The adjustment of the junction before point A2 also involves moderate changes in the Pt−Pt bonds (e.g., d_2). This tendency is inverted beyond A2, where further stretching leads to an increase of α and elongation of d_1 until its full rupture. The richness of possible HJ configurations also allows different conformations for similar electrode distance, which are similar in energy (Supplementary Section 7). Such flexibility can lower the probability for junction rupture during elongation.

To gain insight into the nature of the bond between the benzene and the frontier Pt atoms, we examined the changes in the bond length and angles of benzene in the junction (Figure 4a, M1), with respect to an isolated benzene molecule. In the junction, the C−C bonds of the benzene are elongated by ∼3%, and the hydrogen atoms are shifted from the benzene plane by up to 12°. These changes imply that the carbons are gaining some sp^3 character, instead of the pure sp^2 character in isolated benzene, by creating a new bond with the Pt atom.

Further calculations using the FHI-aims package[40] were performed in order to learn about the orbitals participating in the benzene−Pt bond (Supplementary Section 6). Examining the relative contributions of Pt and benzene orbitals to the Kohn−Sham (KS) eigenstates of a cluster containing benzene in between two Pt electrodes allows for determining their importance to the bond. Two configurations were examined: without additional atoms (similar to M1 in Figure 4a) and with two additional atoms on one side (similar to A1 in Figure 4c). In both cases, the cluster eigenstates (e.g., Figure 5), when projected on Pt apex atoms, have a strong d character, where the contribution of d_z^2 is usually less significant. s and p orbital contributions were also smaller than that of the d orbitals. This is in contrast to the case of Pt monatomic chains, where s and d_z^2 are the dominant orbitals in the Pt−Pt bond.[41] Considering the benzene contribution, the four valence π orbitals (two HOMOs and two LUMOs) play a significantly stronger role than the other orbitals. Thus, the Pt-benzene bond is mainly based on $d-\pi$ hybridization, as can also be inferred by inspection of the eigenstates presented in Figure 5. Furthermore, most of the eigenstates are spread over both the benzene and the electrodes, revealing electron delocalization over the whole structure. The strong Pt-benzene hybridization is also apparent from the mixing of both HOMO and LUMO π orbitals of the benzene into individual eigenstates (e.g., Figure 5b).

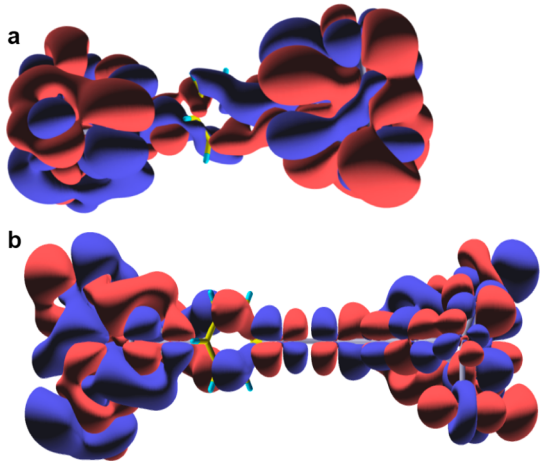

Figure 5. Examples of calculated KS eigenstates of Pt/benzene clusters corresponding to two types of Pt/benzene junctions: without additional atoms (a) and with two additional atoms on one side of the benzene (b). The presented eigenstates have energies of ∼0.01 eV and ∼0.125 eV below the HOMO, respectively. These representative eigenstates are delocalized over the whole Pt/benzene structure. Both of them arise from hybridization mainly between the π antisymmetric HOMO of the benzene with the d_{xy} orbital of the Pt apex atoms. In b there is also some contribution from the π antisymmetric LUMO of the benzene.

To conclude, we have found that benzene and other organic molecules can be electrically wired by chains of Pt atoms, while maintaining high conductance that is insensitive to additional chain elongation once the hybrid is formed. The length of HJs based on benzene depends on the applied voltage, and at sufficiently low voltage, it can exceed the length of pure Pt atomic chains formed at the same conditions. Calculations show that the benzene based HJ is energetically stable and has considerable structural freedom with some energetic preference to HJs with a single chain. The studied HJs demonstrate how individual organic molecules can be wired by the smallest available conducting wire. This is a further step toward more versatile atomic-scale electronic conductors that combine the different worlds of metallic and molecular nanostructures. The HJs form a fascinating class of heterogeneous interfaces between two different low-dimensional systems that can serve as an attractive playground for electronic and heat transport at the atomic scale.

■ ASSOCIATED CONTENT

Supporting Information

Experimental and data analysis details; theoretical methods; asymmetric coupling observation by inelastic electron spectroscopy. This material is available free of charge via the Internet at http://pubs.acs.org.

■ AUTHOR INFORMATION

Corresponding Author

*E-mail: oren.tal@weizmann.ac.il.

Author Contributions

#T.Y. and R.V. contributed equally to this work.

Notes

The authors declare no competing financial interest.

dx.doi.org/10.1021/nl304702z | *Nano Lett.* XXXX, XXX, XXX−XXX

■ ACKNOWLEDGMENTS

O.T. acknowledges support of the Israel Science Foundation Grant No. 1313/10, the German-Israeli Foundation Grant No. I-2237-2048.14/2009 (GIF Young), Minerva Foundation Grant No. 711136 and the Herold Perlman Family. L.K. acknowledges the Israel Science Foundation and the Lise Meitner Minerva Center for Computational Chemistry. F.E. acknowledges funding by the DFG-Center of Functional Nanostructures and by the DFG Priority Program 1243; A.B. acknowledges funding by the DFG (research grant BA 4265/2-1). Furthermore, F.E. and A.B. thank I. Kondov (SCC) for support and the Juelich Supercomputer Center (project HKA12) for allocation of computing time on JUROPA. Finally, F.E. also expresses his gratitude to the IAS of Hebrew University, where part of the work has been performed in the workshop Molecular Electronics, for its warm hospitality.

■ REFERENCES

(1) Nitzan, A.; Ratner, M. A. *Science* **2003**, *300*, 1384−1389.
(2) Elbing, M.; Ochs, R.; Koentopp, M.; Fischer, M.; Von Hänisch, C.; Weigend, F.; Evers, F.; Weber, H. B.; Mayor, M. *Proc. Natl. Acad. Sci. U.S.A.* **2005**, *102*, 8815.
(3) Yu, L.; Keane, Z.; Ciszek, J.; Cheng, L.; Tour, J.; Baruah, T.; Pederson, M.; Natelson, D. *Phys. Rev. Lett.* **2005**, *95*, 256803.
(4) Chen, F.; Li, X.; Hihath, J.; Huang, Z.; Tao, N. *J. Am. Chem. Soc.* **2006**, *128*, 15874−15881.
(5) Martin, C. A.; Ding, D.; Sørensen, J. K.; Bjørnholm, T.; van Ruitenbeek, J. M.; van der Zant, H. S. J. *J. Am. Chem. Soc.* **2008**, *130*, 13198−13199.
(6) Venkataraman, L.; Klare, J. E.; Tam, I. W.; Nuckolls, C.; Hybertsen, M. S.; Steigerwald, M. L. *Nano Lett.* **2006**, *6*, 458−462.
(7) Yanson, A. I.; Bollinger, G. R.; van den Brom, H. E.; Agrait, N.; van Ruitenbeek, J. M. *Nature* **1998**, *395*, 783−785.
(8) Ohnishi, H.; Kondo, Y.; Takayanagi, K. *Nature* **1998**, *395*, 780−783.
(9) Smit, R.; Untiedt, C.; Yanson, A.; van Ruitenbeek, J. *Phys. Rev. Lett.* **2001**, *87*, 266102.
(10) Csonka, S.; Halbritter, A.; Mihály, G. *Phys. Rev. B* **2006**, *73*, 075405.
(11) Kiguchi, M.; Stadler, R.; Kristensen, I.; Djukic, D.; van Ruitenbeek, J. *Phys. Rev. Lett.* **2007**, *98*, 146802.
(12) Thijssen, W. H. A.; Strange, M.; van Ruitenbeek, J. M.; et al. *New J. Phys.* **2008**, *10*, 033005.
(13) Nakazumi, T.; Kiguchi, M. *J. Phys. Chem. Lett.* **2010**, *1*, 923−926.
(14) Kiguchi, M.; Hashimoto, K.; Ono, Y.; Taketsugu, T.; Murakoshi, K. *Phys. Rev. B* **2010**, *81*, 195401.
(15) Makk, P.; Balogh, Z.; Csonka, S.; Halbritter, A. *Nanoscale* **2012**, *4*, 4739−4745.
(16) Wu, S.; Gonzalez, M. T.; Huber, R.; Grunder, S.; Mayor, M.; Schonenberger, C.; Calame, M. *Nat. Nanotechnol.* **2008**, *3*, 569−574.
(17) Xiao, X.; Xu, B.; Tao, N. J. *Nano Lett.* **2004**, *4*, 267−271.
(18) Kim, Y.; Hellmuth, T. J.; Bürkle, M.; Pauly, F.; Scheer, E. *ACS Nano* **2011**, *5*, 4104−4111.
(19) Kim, Y.; Song, H.; Strigl, F.; Pernau, H.-F.; Lee, T.; Scheer, E. *Phys. Rev. Lett.* **2011**, *106*, 196804.
(20) Cheng, Z.-L.; Skouta, R.; Vazquez, H.; Widawsky, J. R.; Schneebeli, S.; Chen, W.; Hybertsen, M. S.; Breslow, R.; Venkataraman, L. *Nat. Nanotechnol.* **2011**, *6*, 353−357.
(21) Huisman, E. H.; Trouwborst, M. L.; Bakker, F. L.; de Boer, B.; van Wees, B. J.; van der Molen, S. J. *Nano Lett.* **2008**, *8*, 3381−3385.
(22) Ferrer, J.; García-Suárez, V. *Phys. Rev. B* **2009**, *80*, 085426.
(23) Muller, C. J.; van Ruitenbeek, J. M.; de Jongh, L. J. *Phys. C (Amsterdam, Neth.)* **1992**, *191*, 485−504.
(24) Tal, O.; Kiguchi, M.; Thijssen, W.; Djukic, D.; Untiedt, C.; Smit, R.; van Ruitenbeek, J. *Phys. Rev. B* **2009**, *80*, 085427.
(25) Agraıt, N.; Yeyati, A. L.; van Ruitenbeek, J. M. *Phys. Rep.* **2003**, *377*, 81−279.
(26) Smit, R.; Untiedt, C.; Rubio-Bollinger, G.; Segers, R.; van Ruitenbeek, J. *Phys. Rev. Lett.* **2003**, *91*, 076805.
(27) Smit, R. H. M.; Noat, Y.; Untiedt, C.; Lang, N. D.; van Hemert, M. C.; van Ruitenbeek, J. M. *Nature* **2002**, *419*, 906−909.
(28) Kiguchi, M.; Tal, O.; Wohlthat, S.; Pauly, F.; Krieger, M.; Djukic, D.; Cuevas, J.; van Ruitenbeek, J. *Phys. Rev. Lett.* **2008**, *101*, 046801.
(29) Shiota, T.; Mares, A.; Valkering, A.; Oosterkamp, T.; van Ruitenbeek, J. M. *Phys. Rev. B* **2008**, *77*, 125411.
(30) García-Suárez, V.; Rocha, A.; Bailey, S.; Lambert, C.; Sanvito, S.; Ferrer, J. *Phys. Rev. Lett.* **2005**, *95*, 256804.
(31) Horsfield, A. P.; Bowler, D. R.; Ness, H.; Sánchez, C. G.; Todorov, T. N.; Fisher, A. J. *Rep. Prog. Phys.* **2006**, *69*, 1195.
(32) Avouris, P. *Acc. Chem. Res.* **1995**, *28*, 95−102.
(33) Smit, R. H. M.; Untiedt, C.; van Ruitenbeek, J. M. *Nanotechnology* **2004**, *15*, S472.
(34) Huang, Z.; Xu, B.; Chen, Y.; Di Ventra, M.; Tao, N. *Nano Lett.* **2006**, *6*, 1240−1244.
(35) Stipe, B. C.; Rezaei, M. A.; Ho, W.; Gao, S.; Persson, M.; Lundqvist, B. I. *Phys. Rev. Lett.* **1997**, *78*, 4410−4413.
(36) Dundas, D.; McEniry, E. J.; Todorov, T. N. *Nat. Nanotechnol* **2009**, *4*, 99−102.
(37) Lü, J.-T.; Brandbyge, M.; Hedegård, P. *Nano Lett.* **2010**, *10*, 1657−1663.
(38) Cruickshank, D. W. J.; Sparks, R. A. *Proc. R. Soc. London, Ser. A* **1960**, *258*, 270−285.
(39) Giannozzi, P.; Baroni, S.; Bonini, N.; Calandra, M.; Car, R.; Cavazzoni, C.; Ceresoli, D.; Chiarotti, G. L.; Cococcioni, M.; Dabo, I.; Dal Corso, A.; de Gironcoli, S.; Fabris, S.; Fratesi, G.; Gebauer, R.; Gerstmann, U.; Gougoussis, C.; Kokalj, A.; Lazzeri, M.; Martin-Samos, L.; Marzari, N.; Mauri, F.; Mazzarello, R.; Paolini, S.; Pasquarello, A.; Paulatto, L.; Sbraccia, C.; Scandolo, S.; Sclauzero, G.; Seitsonen, A. P.; Smogunov, A.; Umari, P.; Wentzcovitch, R. M. *J. Phys.: Condens. Matter* **2009**, *21*, 395502.
(40) Blum, V.; Gehrke, R.; Hanke, F.; Havu, P.; Havu, V.; Ren, X.; Reuter, K.; Scheffler, M. *Comput. Phys. Commun.* **2009**, *180*, 2175−2196.
(41) Nielsen, S.; Brandbyge, M.; Hansen, K.; Stokbro, K.; van Ruitenbeek, J.; Besenbacher, F. *Phys. Rev. Lett.* **2002**, 89.